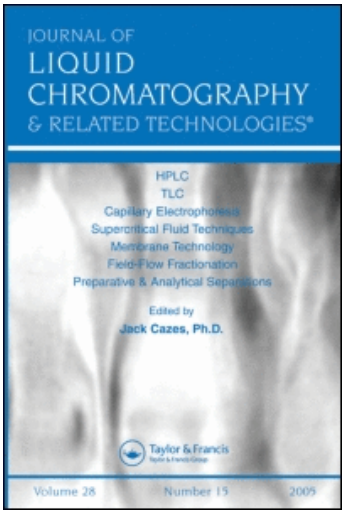

Journal of Liquid Chromatography & Related Technologies
Publication details, including instructions for authors and subscription information:
http://www.informaworld.com/smpp/title~content=t713597273

An Investigation of the Influence of the Gravity Field on the Interface of Two Immiscible Liquids—A Computational Study Comparing Prediction with Experiment

Carola S. König[a]; Ian A. Sutherland[a]
[a] Brunel Institute for Bioengineering, Brunel University, Uxbridge, Middlesex, UK

Online publication date: 29 May 2003

To cite this Article König, Carola S. and Sutherland, Ian A.(2003) 'An Investigation of the Influence of the Gravity Field on the Interface of Two Immiscible Liquids—A Computational Study Comparing Prediction with Experiment', Journal of Liquid Chromatography & Related Technologies, 26: 9, 1521 — 1535
To link to this Article: DOI: 10.1081/JLC-120021264
URL: http://dx.doi.org/10.1081/JLC-120021264

JOURNAL OF LIQUID CHROMATOGRAPHY & RELATED TECHNOLOGIES®
Vol. 26, Nos. 9 & 10, pp. 1521–1535, 2003

An Investigation of the Influence of the Gravity Field on the Interface of Two Immiscible Liquids—A Computational Study Comparing Prediction with Experiment

Carola S. König* **and Ian A. Sutherland**

Brunel Institute for Bioengineering, Brunel University, Uxbridge, UK

ABSTRACT

The flow of two immiscible liquids in a tube was investigated using computational fluid dynamics (CFD). This work is a first step towards investigating the influence of a variable gravitational field on the interface between the upper and lower phase of immiscible solvents as used in counter-current chromatography (CCC). Initially the tube was positioned horizontally with the heavier fluid (lower phase) at the bottom and the lighter fluid (upper phase) on the top. Then the tube was suddenly tilted to a fixed inclination angle α. The flow field was initially exposed to a standard 1g gravity field (case 1). Subsequently,

*Correspondence: Carola S. König, Brunel Institute for Bioengineering, Brunel University, Uxbridge, Middlesex, UB8 3PH, UK; E-mail: carola.koenig@brunel.ac.uk.

DOI: 10.1081/JLC-120021264
1082-6076 (Print); 1520-572X (Online)

MARCEL DEKKER, INC.
270 Madison Avenue, New York, New York 10016

runs for a 2*g* and 10*g* gravity vector were performed (cases 2 and 3, respectively). Predictions for case 1 compared favorably with experimental results, although it was noted that there was a slight time slippage. The numerical results for the cases 2 and 3 showed that the higher the gravitational force the sooner distinct waves occur at the interface and the more disturbed the interface becomes in time. The interface surface area becomes minimal more quickly in the high gravity case due to the fluids moving more quickly to their respective ends, hence reducing the time when mass transfer between the phases is possible. However, mass transfer is still likely to have been enhanced due to the better mixing as a result of the highly disturbed interface. These encouraging results indicate that CFD could become a powerful tool in understanding the complex nature of the fluid dynamics in coil planet centrifuges and countercurrent chromatography.

Key Words: Computational study; Interface; Gravity field; Numerical model; CFD; Experiment; Visualization; Two-phase flow; Stratified; Immiscible liquids.

INTRODUCTION

Differences between the physical properties of the products that are contained in a mixture of two immiscible solvent phases form the basis for many separation methods. Some methods rely on the differences in partitioning of the products between two such phases, as is the case in liquid–liquid extraction and partition chromatography. Counter-current chromatography (CCC) is a form of liquid–liquid chromatography that combines the advantages of both methods. The process takes place along a continuous length of tubing. One phase is held stationary, while the other is pumped through it in such a way that there is good retention of the stationary phase. A series of simultaneous mixing and settling zones occur along the length of the tubing. The mixing and settling process and the mass transfer between the phases are the key elements for successful high-resolution liquid–liquid chromatography.[1] In CCC continuous tubing is wound on a drum, which is rotated in planetary motion. Hence the two-phase system is exposed to an unsteady high gravity field, thus a sample injected into the mobile phase will experience a number of mixing and settling steps according to the set rotor speed. Although phase distribution and phase-mixing phenomena, which are fundamental to CCC, are directly linked to the experienced gravity field, its influence is still poorly understood.[1–3]

As a first step to investigating the influence of the gravity field on the interface between the upper and lower phase in CCC, the flow of two

Marcel Dekker, Inc.
270 Madison Avenue, New York, New York 10016

immiscible liquids in a tube was investigated using computational fluid dynamics (CFD). The latter allows manipulation of applied body forces such as buoyancy force and rotational forces.

The sudden exposure of a tube containing stratified, immiscible liquids (of different density and viscosity) to gravity under an angle results in a flow with shear at the interface. Flow of this form is susceptible to instabilities of various kinds.[4,5] Thorpe[6–8] carried out groundbreaking experimental and theoretical work on this type of flow.

METHODOLOGY

Experimental Model

The experimental model was made of a cylindrical glass tube 0.5 m long with an internal diameter of 10 mm. The ends of the tube were closed and square-ended. The tube was filled with the upper and lower phase (each 50% by volume) of a heptane/ethyl acetate/methanol/water phase system (phase system 4B[1]). Before the tube was filled, the density ρ and viscosity μ of the phases were measured along with the interfacial tension σ at 30°C ($\rho_{\text{upper}} = 713.68\,\text{kg m}^{-3}$, $\mu_{\text{upper}} = 0.3549\text{E-}3\,\text{kg m}^{-1}\,\text{s}^{-1}$, $\rho_{\text{lower}} = 923.84\,\text{kg m}^{-3}$, $\mu_{\text{lower}} = 1.3406\text{E-}3\,\text{kg m}^{-1}\,\text{s}^{-1}$, $\sigma = 6.0569\text{ E-}3\,\text{N m}^{-1}$). Initially, the tube was horizontal with the upper phase on the top and the lower phase at the bottom. Then the tube was suddenly tilted to a fixed inclination angle of 15° around its centre (see Fig. 1). When the tube had reached its fixed position, the timing was started allowing 0.1 s for the actual rotation. The flow was filmed with a digital video camera (model GY-DV500 by JVC) at standard framing rate.

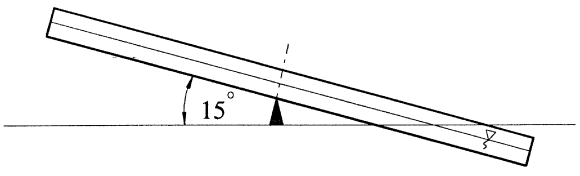

Figure 1. Initiation of the flow: the pipe is suddenly tilted to a fixed inclination angle of 15°.

MARCEL DEKKER, INC.
270 Madison Avenue, New York, New York 10016

Numerical Model

The numerical model is a two-dimensional representation of the experimental model. The grid of the numerical model is block-structured consisting of two blocks and 64,000 cells. Initially the flow field was exposed to a standard 1*g* gravity field (case 1). Subsequently, runs for a 2*g* and 10*g* gravity vector were performed (cases 2 and 3). In all cases the gravity vector was applied to the horizontally positioned tube at an angle of 15°.

The unsteady two-phase fluid flow is treated as two-dimensional, laminar, Newtonian, isothermal, and buoyant. In this study the governing equations were solved using the code CFX-4 (release 4.3) by AEA Industrial Technology, Harwell, UK. A homogenous two-fluid model based on mass and momentum conservation was used. Here the individual phase continuity equations are solved to determine the volume fractions. The individual transport equations are summed over all phases to give a single transport equation. The code models the surface tension force based on the continuum surface model of Brackbill et al.[9] To avoid a smeared interface, that may develop due to numerical diffusion in time, a surface sharpening algorithm was employed.[10]

Each time step uses the solution (phase volume fractions, velocities, and pressure) of the previous time step as initial conditions. The pressure was obtained using the SIMPLEC algorithm. The differencing schemes used are a fully implicit backward differencing procedure for time, central differencing for pressure, upwind differencing for the phase volume fractions and hybrid differencing for the velocity variables. The under-relaxation factors were set to 0.65 for the velocity components and the volume fractions and to 1.0 for the pressure. The runs were performed for a wall contact angle of 90° (as an initial approximation). The surface sharpening level was set to 2. For the cases 1 and 2 each computational time step was 10 ms. For case 3 the time step was reduced to 5 ms. However, the results were dumped every 100 ms. Each time step was calculated for a fixed number of iterations. The minimum reduction of the mass source residuals per time step was one order of magnitude. The achieved total mass source residuals were of the order of 1E-5 $kg\,s^{-1}$. At this point in the computation the residuals for the velocity components and the volume fractions were also reduced to acceptable levels.

THEORETICAL VALIDATION DATA

The capillary wave length is a common means to describe the microscopic behavior at the interface between two immiscible liquids. It represents the

wave length of the deformations that may occur at the interface of the two liquids. It compares the relative intensities of interfacial tension forces, which tend to smooth all deformations at the interface, and of gravity forces, which have the reverse effect[11]. It is defined as

$$\lambda_{\text{cap}} = 2\pi\sqrt{\frac{\sigma}{|\Delta\rho|g}} \tag{1}$$

where σ is the interfacial tension, $\Delta\rho$ is the density difference between the two phases, and g is the gravitational acceleration. In the Kelvin–Helmholtz

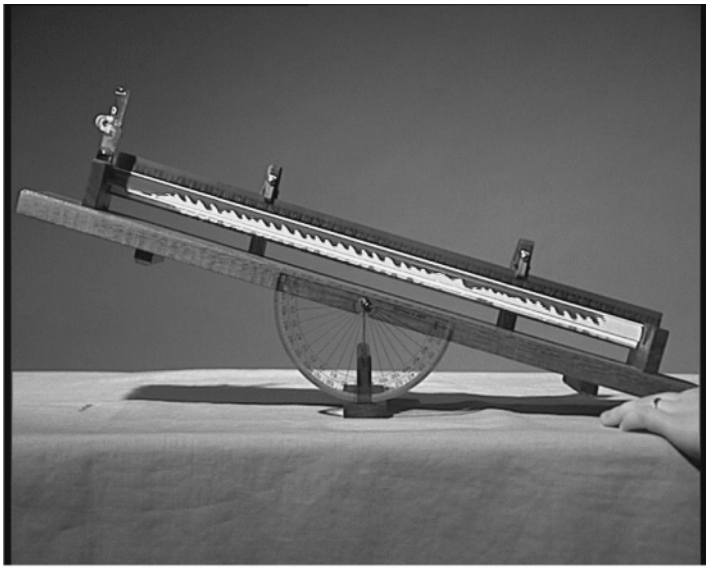

a)

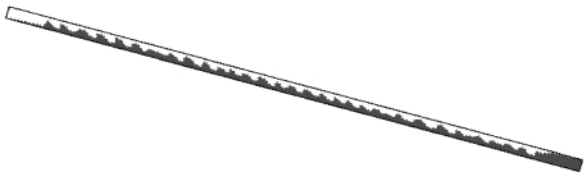

b)

Figure 2. Interface distribution for case 1 at approximately $t = 0.5$ s: (a) experiment; (b) simulation.

MARCEL DEKKER, INC.
270 Madison Avenue, New York, New York 10016

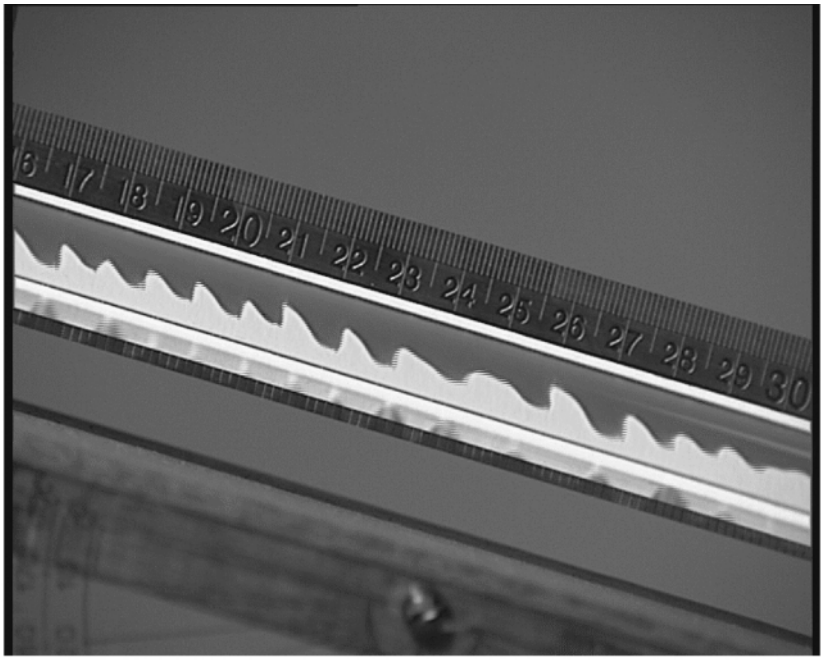

a)

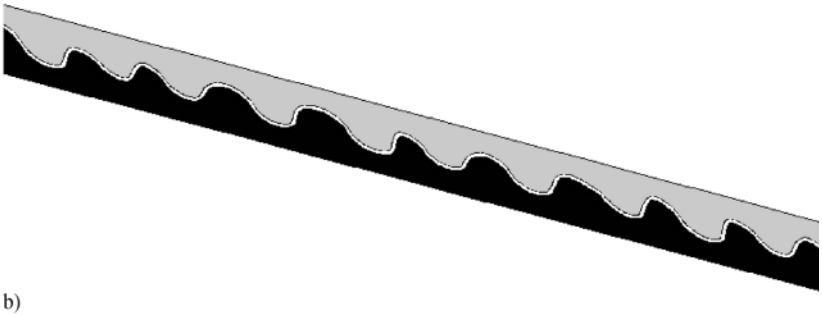

b)

Figure 3. Interface distribution for case 1 in the central section at approximately $t = 0.5$ s: (a) experiment; (b) simulation.

MARCEL DEKKER, INC.
270 Madison Avenue, New York, New York 10016

stability criterion,[7,12,13] the capillary wave length is also known as the critical wave length.

RESULTS AND DISCUSSION

Unit Gravity (Case 1)

When the tube was suddenly rotated to the fixed inclination angle in the experiments, no initial motion or instability could be observed for $t < \sim 0.3$ s. Therefore, good agreement with the numerical simulation, where the flow field is exposed to the gravitational force instantaneously, was expected. In the centre of the tube the flow, starting from rest, is initially parallel to the tube walls. Soon after the first instabilities can be observed at the interface, a distinct wave pattern forms along the entire interface. This is shown in both, the experiment and the numerical simulation in Fig. 2 for the entire tube at $t = 0.5$ s. (Please note that in the experimental image the tube diameter appears to be optically larger because of the tube wall thickness and some reflections at the bottom.) Figure 3 shows the interface distribution at the same instant in detail in the central section.

Evaluating Eq. (1) for the phase system 4B, results in a value of 10.8 mm for λ_{cap}. While the experimental values for λ_{cap} were slightly lower than this showing quite some variation ranging between approximately 7.2 and 10.8 mm, the simulation values for λ_{cap} were slightly over-predicted ranging from approximately 10.8 to 14.2 mm. Some of the differences for λ_{cap} between the numerical simulation and the experiment may be attributed to differences between the experimental and numerical models. The measured values for density, viscosity, and interfacial tension may have been slightly different while filming the experiment with the tube strongly illuminated. However, it is believed that the influences of these changes are only minor as a numerical test run with the properties of phase system 4B as referenced in[1] resulted only in very small differences for λ_{cap}. In the three-dimensional experimental model, however, the additional wall effects may have a significant effect on the wave length. One possible way of compensating for this may be to choose the height of the two-dimensional model to be the height of an equivalent area square section. Alternatively, a three-dimensional model may prove necessary.

Figure 4 shows the interface distribution in the centre region 0.4 s later than for the situation in Fig. 3. The numerical simulation and experiment compare very favorably. Figure 5 shows a droplet breaking off the tip of the highly undercut wave of Fig. 4 in the simulation at $t = 1.0$ s. As the flow further progresses differences in the interface distribution increase. In

MARCEL DEKKER, INC.
270 Madison Avenue, New York, New York 10016

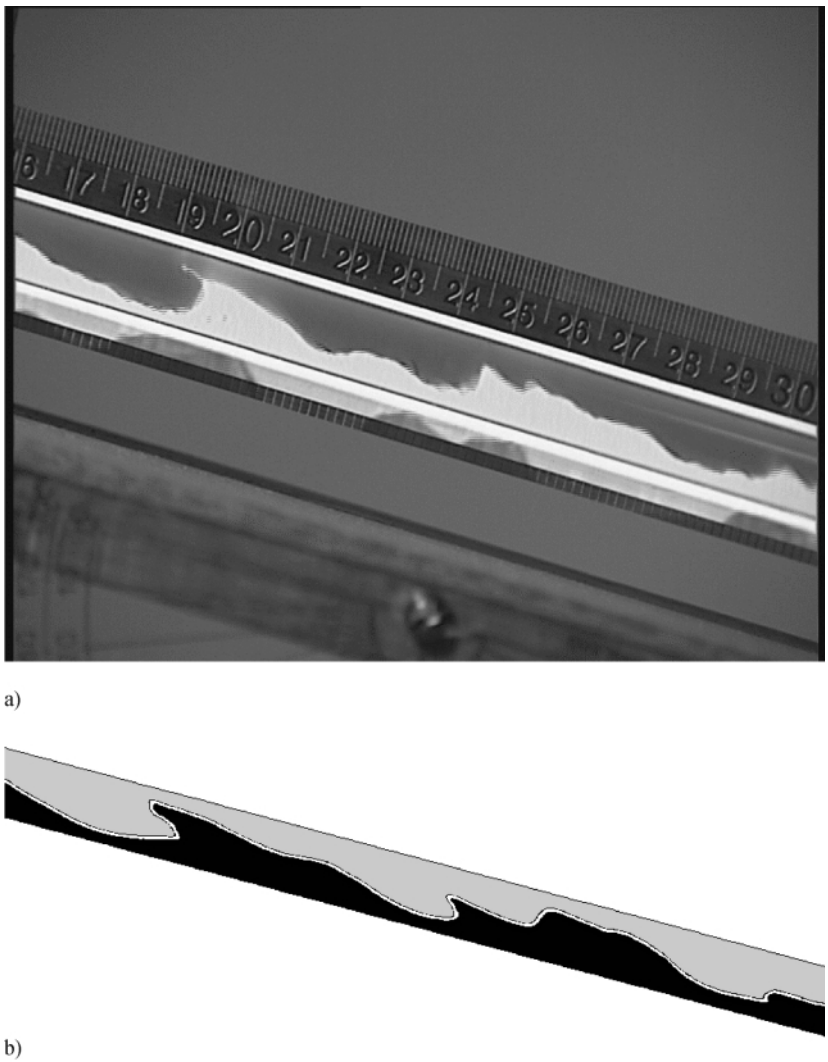

Figure 4. Interface distribution for case 1 in the central section at approximately $t = 0.9$ s: (a) experiment; (b) simulation.

MARCEL DEKKER, INC.
270 Madison Avenue, New York, New York 10016

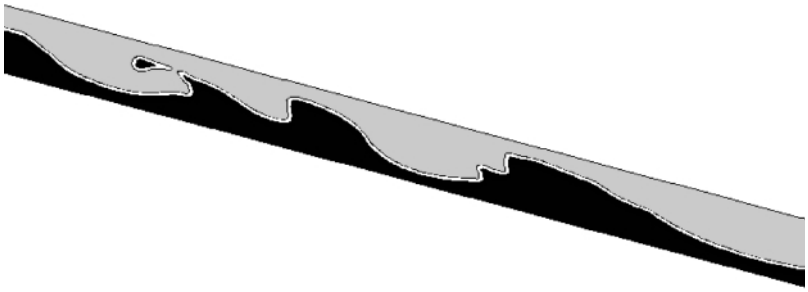

Figure 5. Interface distribution for case 1 in the central section in the stimulation at $t = 1.0$ s.

the simulation there is a greater trend for droplet formation as shown in Fig. 6(b) at $t = 1.4$ s. This may again be as a result of the differences in the model as discussed above but also, it may be partly due to numerical diffusion. The predicted interface at $t = 1.6$ s in Fig. 7 would compare better with Fig. 6(a). As the flow further progresses, the upper and lower phases eventually occupy the respective halves of the tube. Figure 8 shows the interface distributions in the final stages before the flow comes to rest. The total time it takes from initiating the flow until the meniscus comes to a halt is on average 4.2 s (± 0.2 s) in the experiment, compared to about 4.6 s in the simulation [not including the time for any remaining droplets attached to the tube wall to be absorbed at the interface, see Fig. 8(b)]. The length in the tube occupied by the interface is not predicted well during the later stages of the flow when the interfacial behavior can become quite random. Distinct interface formations do not necessarily occur at the same instant, however, they agree well in shape. In the last stage of the flow the meniscus was seen notably oscillating about four times before coming to rest in the experiment. This oscillation was seen only about twice in the simulation (not counting any further oscillations caused by droplet absorption). This may again be as a result of the differences between the numerical and experimental models as discussed above. It should also be noted that after the distinct wave pattern forms along the entire interface in the early stages, the highly unstable nature of the flow results in notable differences in the interface distribution when repeating the experiment under the same conditions.

MARCEL DEKKER, INC.
270 Madison Avenue, New York, New York 10016

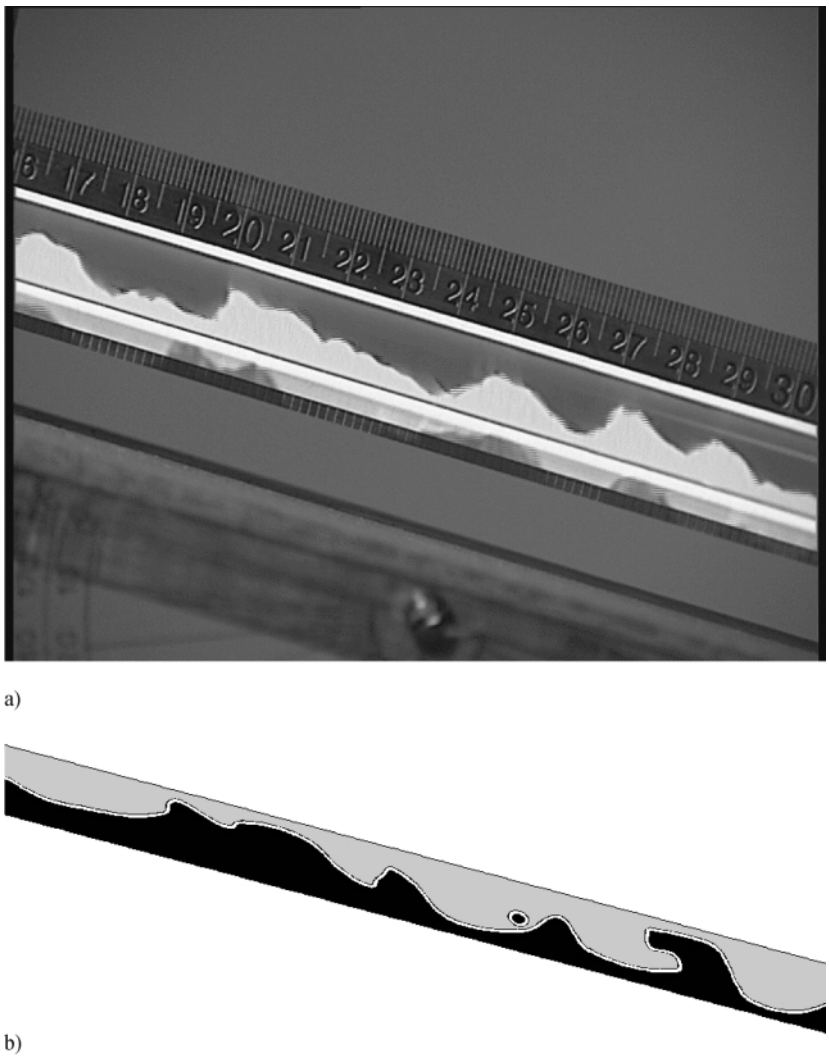

a)

b)

Figure 6. Interface distribution for case 1 in the central section at approximately $t = 1.4$ s: (a) experiment; (b) simulation.

MARCEL DEKKER, INC.
270 Madison Avenue, New York, New York 10016

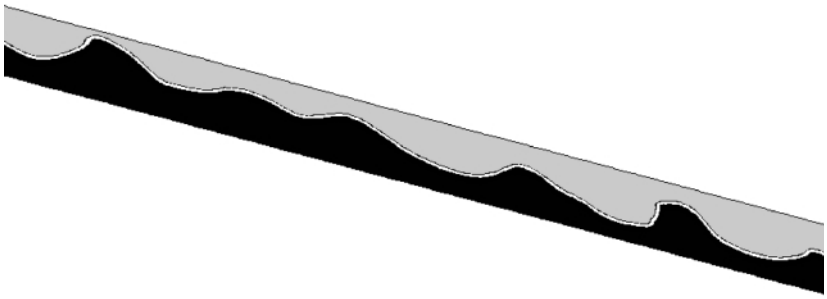

Figure 7. Interface distribution for case 1 in the central section in the simulation at $t = 1.6$ s.

Enhanced Gravity (Cases 2 and 3)

Figures 9 and 10 show the initial interface development for the $2g$ and $10g$ vector field, respectively. As expected the interface formed varies significantly for the three different gravity fields. While for the $1g$ field a regular wave formation can be seen clearly at $t = 0.5$ s [Fig. 3(b)], such disturbances are seen already at $t = 0.4$ s for the $2g$ field [Fig. 9(a)] and at $t = 0.2$ s for the $10g$ field [Fig. 10(b)]. The higher the gravitational force, the sooner distinct waves occur at the interface. The undercut of the waves is most pronounced for the highest g field, as shown in Fig. 10(b). Wave breakage and droplet formation are much increased for the $10g$ field and were observed very soon after initiation of the flow as shown in Fig. 10(c). Also, it was observed that the higher the g field the flatter the resulting meniscus shape was (not shown) and boundary contact effects were reduced. While it takes approximately 4.6 s from initiating the flow until the meniscus comes to a halt for case 1, it takes about 3.5 s and 1.6 s for the cases 2 and 3, respectively. Although the interface surface area becomes minimal more quickly in the high gravity case due to the fluids moving more quickly to their respective ends, hence reducing the time when mass transfer between the phases is possible, mass transfer is still likely to have been enhanced due to the better mixing as a result of the highly disturbed interface.

CONCLUSIONS

The numerical results for case 1 compared overall favorably with experimental results, although a slight time slippage was observed. One of

Marcel Dekker, Inc.
270 Madison Avenue, New York, New York 10016

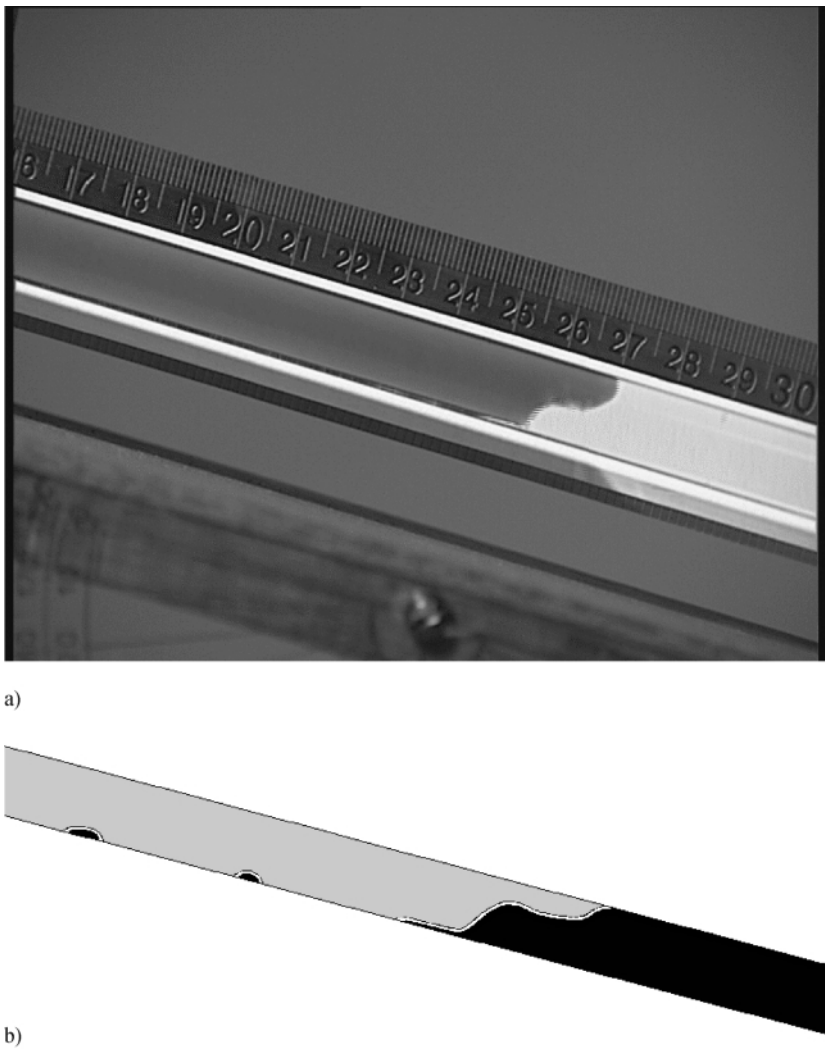

Figure 8. Interface distribution for case 1 in the central section: (a) experiment at approximately $t = 3.1$ s; (b) simulation at $t = 3.7$ s.

Marcel Dekker, Inc.
270 Madison Avenue, New York, New York 10016

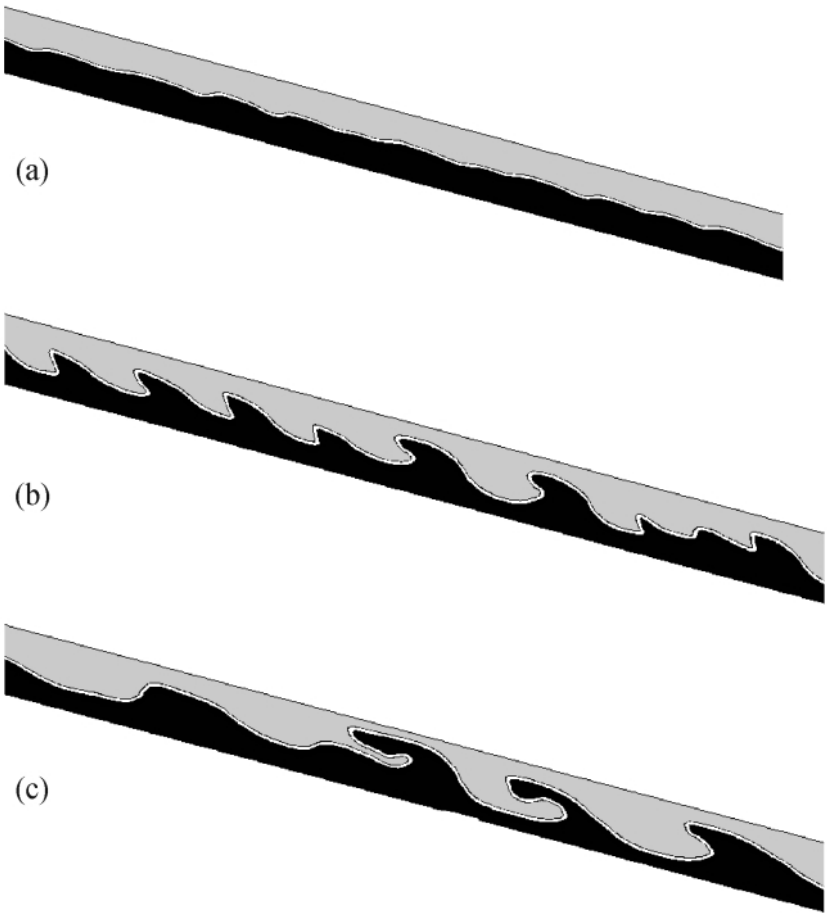

Figure 9. The developing interface for the $2g$ vector field in the central section at (a) $t = 0.3$ s; (b) $t = 0.4$ s; and (c) $t = 0.5$ s.

the main reasons for the differences seen between the numerical and experimental results is likely to be the three-dimensionality of the experimental model. Also, numerical diffusion may have contributed to these differences. The numerical results of cases 2 and 3 demonstrate the significance of the gravity field on the interface distribution between two phases. Its actual influence on mass transfer will need further investigation. This study allows the conclusion that the CCC process can be better understood and improved using CFD. Further research will allow for the studying of mass

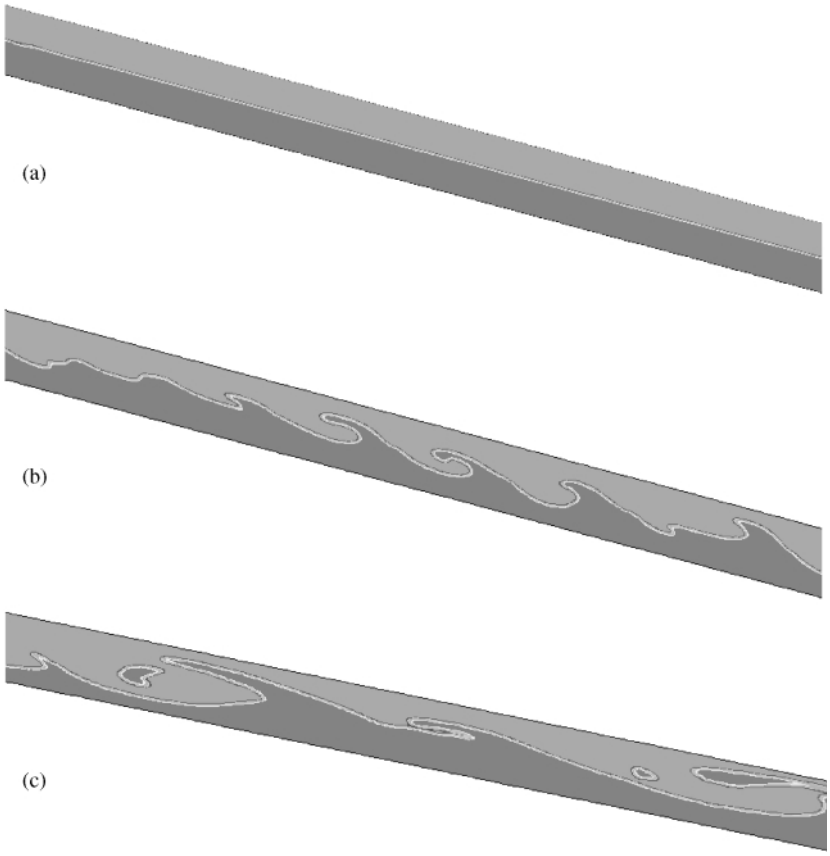

Figure 10. The developing interface for the 10*g* vector field in the central section at (a) $t = 0.1$ s; (b) $t = 0.2$ s; and (c) $t = 0.3$ s.

transfer between phases and will include the development of a single coil model. The latter will also allow for the typical cyclic acceleration fields as encountered in coil planet centrifuges.

REFERENCES

1. Sutherland, I.A.; Muytjens, J.; Prins, M.; Wood, P. A new hypothesis on phase distribution in countercurrent chromatography. J. Liq. Chrom. & Rel. Technol. **2000**, *23* (15), 2259–2276.

Marcel Dekker, Inc.
270 Madison Avenue, New York, New York 10016

2. Conway, W.D. *Countercurrent Chromatography: Apparatus, Theory and Applications*; VCH Publishers: Weinheim, Germany, 1990, ISBN 0-89573-331-5.
3. Wood, P.L.; Jaber, B.; Sutherland, I.A. A new hypothesis on the hydrodynamic distribution of the upper and lower phases in CCC. J. Liq. Chrom. & Rel. Technol. **2001**, *24* (11&12), 1629–1654.
4. Boomkamp, P.A.M.; Miesen, R.H.M. Classification of instabilities in parallel two-phase flow. Int. J. Multiphase Flow **1996**, *22*, 67–88.
5. Ishii, M. Wave phenomena and two-phase flow instabilities. In *Handbook of Multiphase Systems*; Hetsroni, G., Ed.; Hemisphere Publishing Corporation, McGraw-Hill: New York, 1982, ISBN 0-07-028460-1, 2-95–2-122.
6. Thorpe, S.A. A method of producing a shear flow in a stratified fluid. J. Fluid Mech. **1969**, *32* (4), 693–704.
7. Thorpe, S.A. Experiments on the stability of stratified shear flows. Radio Sci. **1969**, *4* (12), 1327–1331.
8. Thorpe, S.A. Experiments on the instability of stratified shear flows: immiscible fluids. J. Fluid Mech. **1969**, *39* (1), 25–48.
9. Brackbill, J.; Kothe, D.B.; Zemach, C. A continuum method for modelling surface tension. J. Comp. Phys. **1992**, *100*, 335–354.
10. Anonymous, CFX-4 Release 4.3. *Solver Manual.* CFX International, Harwell Laboratory: Oxfordshire, UK.
11. Menet, J.-M.; Rolet-Menet, M.-C. Characterization of the solvent systems used in countercurrent chromatography. In *Countercurrent Chromatography*; Chromatogr. Sci. Ser.; 1999; Vol. 82, 1–28.
12. Helmholtz, H. *Über discontinuierliche Flüssigkeitsbewegungen*; Monatsber. Deutsch. Akad. Wiss.: Berlin, 1868; 215–228.
13. Kelvin, L. Hydrokinetic solutions and observations. Phil. Mag. **1871**, *4* (42), 362–377.

Received June 24, 2002
Accepted November 30, 2002
Manuscript 6044L

MARCEL DEKKER, INC.
270 Madison Avenue, New York, New York 10016